

Dorota Biniś\*,  
Włodzimierz Biniś,  
Jarosław Janicki

# Application of Raman Spectroscopy for Evaluation of Chemical Changes in Dibutrylchitin Fibres

DOI: 10.5604/12303666.1207842

University of Bielsko-Biala,  
Institute of Textile Engineering  
and Polymer Materials  
ul. Willowa 2, 43-309 Bielsko-Biala, Poland;  
\*E-mail: dbinias@ath.bielsko.pl

## Abstract

*Microporous dibutrylchitin (DBC) fibres formed by means of a dry-wet method were treated with aqueous solutions of potassium hydroxide. By applying various parameters of the alkaline treatment, fibres can be transformed into fibres from regenerated chitin or even into chitosan fibres. In the first stage, with the application of 5% KOH solutions and temperatures ranging from 20 to 90 °C, fibres from regenerated chitin were obtained. The subsequent treatment stage with saturated KOH solutions and the temperature range 70 - 140 °C resulted in obtaining fibres from chitosan with different deacetylation degrees. Structural changes in the fibres occurring in the course of their chemical treatment were analysed using RAMAN spectroscopy. Raman spectra were next mathematically processed by means of GRAMS software within the range 1800 - 820 cm<sup>-1</sup> in order to evaluate the changes quantitatively. A new method is described for the determination of butyrylation and deacetylation degrees of dibutrylchitin, chitin and chitosan. Analysis of the fibres obtained carried out by means of RAMAN spectroscopy proves that in the process gradual degradation of the polymer chains takes place.*

**Key words:** Raman spectra, dibutrylchitin fibres, deesterification degree, chitin fibres, deacetylation degree.

## ■ Introduction

Chitin (poly-(1-4)-2-acetamido-2-deoxy-D-glucopyranose) is a natural polymer formed in a biosynthesis process. Like cellulose, chitin is a polysaccharide with a ring-structure polymer chain. Chitin is present in the shells of sea crustacea (shrimps, crabs, krill, lobsters). It can also be found in insects, as well as in some microorganisms and fungi [1, 2]. The interest in chitin and its derivatives mainly results from the fact that these materials possess specific properties, such as biocompatibility, bioactivity and biodegradability, which makes them useful for biomedical purposes [3]. As a renewable material, chitin offers many potential applications in a number of fields, ranging from wastewater treatment, cosmetics, drug delivery, artificial skin, and many other novel applications [4].

Chitin is characterised by its molecular weight and degree of crystallinity. The potential application of chitin is related to its crystalline structure and thermal properties [3, 5]. Chitin is insoluble in water and most organic solvents. It is, however, soluble in a few compounds such as inorganic acids, highly concentrated formic acid and N,N-Dimethylacetamide/lithium chloride (DMAc-LiCl), hexafluoroacetone or hexafluoro-2-propanol [6]. However its low solubility makes it difficult to process, and thus significantly limits the application of chitin.

Thermal stability, which can be analysed using differential scanning calorimetry (DSC) and thermal gravimetric analysis (TGA) techniques, is a critical factor for determining the potential applications of chitin and its derivatives [5].

Therefore different physical and chemical modifications are carried out in order to obtain chitin derivatives with considerably better solubility, maintaining at the same time the biological activity of chitin [7]. The basic derivative of chitin is chitosan, generally produced by alkaline deacetylation of chitin. It displays valuable specific properties such as biodegradability, bioactivity, biocompatibility and nontoxicity [8 - 10]. Chitosan is applied to many fields such as medicine and medical dressings applied on wounds, scalds and as a solid support for medicine to control release, and it also acts as hydrogel [11, 12].

Etherification is one of the most important modifications used to prepare water soluble chitin derivatives, containing carboxymethylchitin and hydroxypropylchitin [13 - 18]. Dibutrylchitin (DBC) is easily soluble in many solvents like dimethyl sulfoxide (DMSO), ethyl alcohol and dimethylformamide (DMF), and has both film and fibre-forming properties [17 - 21]. The properties of DBC creates the possibility of manufacturing a wide assortment of DBC materials suitable for medical applications. Investigations

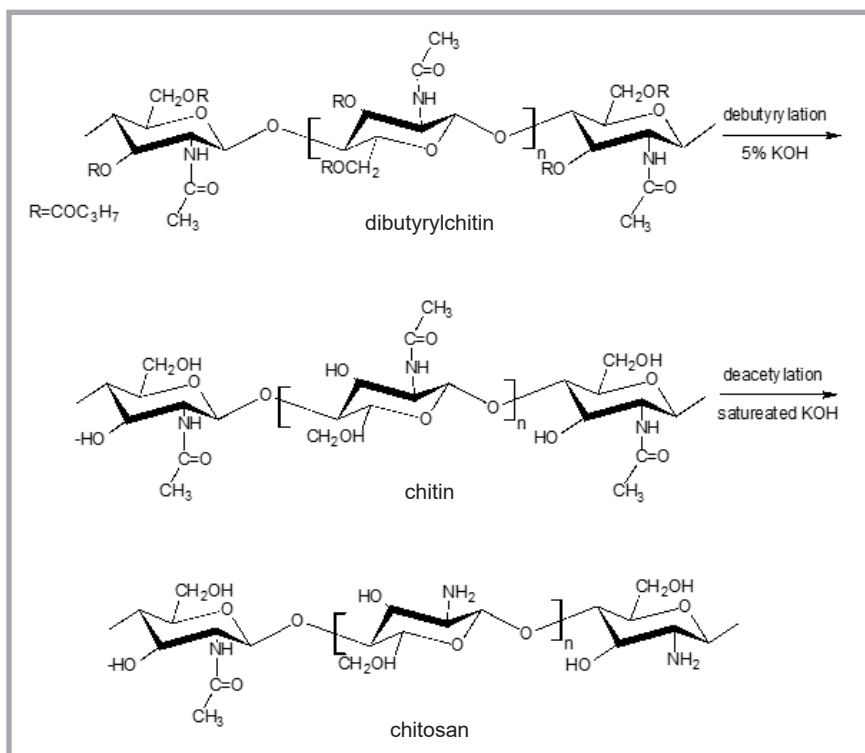


**Figure 1.** Reaction scheme of the hydrolysis of DBC by chitin and for the process deacetylation process of regenerated chitin to the chitosan.

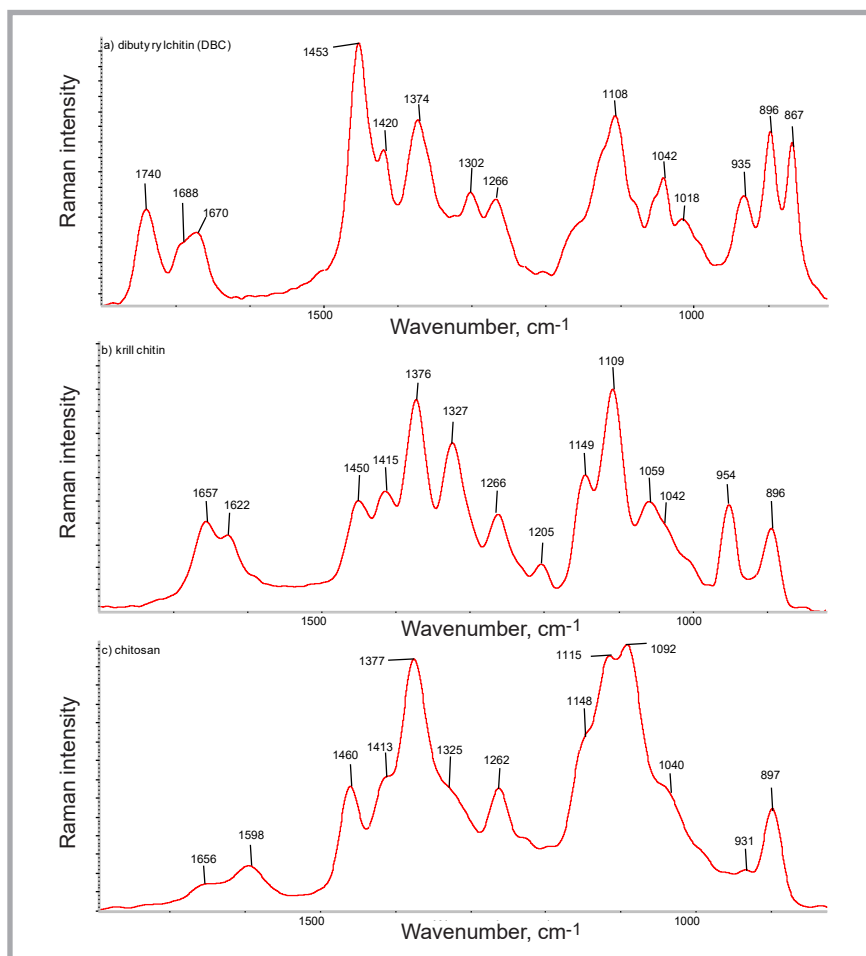


**Figure 2.** Set of FT Raman spectra for a) dibutyrilchitin (DBC), b) krill chitin and c) chitosan (DD – 90%) within the range 1800 – 820  $\text{cm}^{-1}$  with the marked characteristic oscillation bands [43 - 46, 48, 50, 51].

of the biological properties of DBC materials, carried out *in vitro* and *in vivo* accordingly, showed good biocompatibility. The excellent biomedical properties of DBC are confirmed by different experimental results which prove that it is a biocompatible and biodegradable polymer [22 - 31].

For example the main technique of analysis of changes in the chemical structure of polymers uses Fourier Transform Infra Red (FTIR). Chitin and chitosan have also been studied extensively by Infrared (IR) spectroscopy [32 - 37].

Characterisation of the chemical structure of dibutyrilchitin is done by using the FTIR technique, reviewed in literature [18, 26, 38 - 40, 42]. The specific chemistry and orientation of the structures known from Raman spectroscopy. Chitin and other derivatives have also been studied by Raman spectroscopy [33, 41 - 43, 45 - 48]. The application of infrared and Raman spectroscopy for evaluation of structural changes in dibutyrilchitin has also been studied [39, 41]. Solid-state structural changes in the resulting chitin fibres were characterised by Raman spectroscopy. Changes in the deesterification degree and deacetylation degree (DA) were also measured [20, 39, 41].

These well-established spectroscopic techniques were used within the present work in order to comprehensively characterise the structural changes by alkali treatment of dibutyrilchitin, chitin and chitosan. This work presents chemical changes in fibres occurring in the course of their chemical treatment, analysed using Raman spectroscopy.

## Experimental

### Materials

#### Materials

Krill chitin –  $(\text{C}_8\text{H}_{13}\text{O}_5\text{N})_n$  (Euphausia superba) according to technology developed at the Sea Fisheries Institute in Gdynia, Poland [49]. Chitosan –  $(\text{C}_6\text{H}_{11}\text{O}_4\text{N})_n$  a commercial product of Vanson supplied by Vanson Halo Source, USA, deacetylation degree 90% and viscometric average molecular weight  $M_v = 346.0$  kDa. Dibutyrilchitin (DBC)  $(\text{C}_{14}\text{H}_{27}\text{O}_7\text{N})_n$  - (synthesised at the Department of Physical Chemistry of Polymers, Lodz University of Technology,  $M_w = 160$  kDa. DBC, obtained by the es-

terification process with krill chitin using butyric anhydride ((CH<sub>3</sub>CH<sub>2</sub>CH<sub>2</sub>CO)<sub>2</sub>O) (Aldrich, USA), and as the catalyst of the reaction perchloric acid (70% HClO<sub>4</sub>) (Merck, USA), ethyl alcohol (C<sub>2</sub>H<sub>5</sub>OH) (POCH, Poland), potassium hydroxide (KOH) – (POCH, Poland).

### Preparation of fibres

In this study, dibutrylchitin prepared as above was next dissolved in anhydrous ethyl alcohol, and a concentrated solution was prepared. DBC fibres were spun using a wet–dry method. The fibres, partly solidified, were then introduced into a water bath and taken up on a bobbin device, stretched twice and next dried in air [19, 20].

### Alkaline treatment of DBC fibres

In the next stage of the investigation, DBC fibres were subjected to alkaline treatment with a 5% KOH solution at temperatures of 20, 50, 70 and 90 °C, which caused their gradual transition to regenerated chitin fibres.

The duration of chitin regeneration from DBC at 20, 50, 70 and 90 °C (series A, B, C and D, respectively) by means of 5% KOH solutions depends on the temperature of the alkaline treatment. The process carried out at room temperature is almost complete after 120 min, while the same process at 90 °C takes only 10 min. Deacetylation was applied for the fibres made of regenerated chitin and for the DBC fibres. Deacetylation reactions were carried out in solutions of potassium hydroxide saturated at definite temperatures, i.e. at 70 °C – series N C (chitin fibres), at 70 °C – series N D (DBC fibres), at 100 °C – series N F (chitin fibres), at 120 °C – series N G (chitin fibres), and at 140 °C – series N H (chitin fibres). When each reaction was completed, the fibres were rinsed several times with ethyl alcohol [39, 40]. A possible reaction scheme of the hydrolysis of dibutrylchitin and for the process deacetylation of regenerated chitin to chitosan are illustrated in **Figure 1**, showing the dibutrylchitin (DBC) chemical structure after debutyrylation (regenerated chitin) and deacetylation (chitosan).

### Analytic methods

#### Measurements in the range of medium FT Raman

All measurements were carried out using an FTIR spectrometer of the MAG-

**Table 1.** Wavenumbers of the bands observed in the FT-Raman spectra of dibutrylchitin, chitin and chitosan bands [43-46, 48, 50, 51]. Samples shown in **Figure 2**.

Sample	Wavenumber from Raman shift, cm <sup>-1</sup>	Oscillation bands
dibutrylchitin	1740	C-O (esters)
	1688	C-O (Amide I)
	1670	N-H (Amide I)
	1453	C-H (def. asym.)
	1420	C-H (def. sym.)
	1374	C-N (stretch.)
	1302	C-H (def. in plane)
	1266	C-H (def. in plane)
	1108	C-O-C (ether.)
	1042	C-O-C (ring)
	1018	C-O (stretch.)
	935	C-H (def. out plane)
	896	C-H (def. out plane)
	867	C-O-C (esters)
	krill chitin	1657
1622		N-H (Amide I)
1450		C-H (def. asym.)
1415		C-H (def. sym.)
1376		C-N (stretch.)
1327		C-H (def. in plane)
1266		C-H (def. in plane)
1149		C-O (stretch.)
1109		C-O-C (ether.)
1059		C-O-C (ring)
1042		C-O (stretch.)
954		C-H (def. out plane)
896		C-H (def. out plane)
chitosan	1656	C-O (Amide I)
	1598	N-H (Amide I)
	1460	C-H (def. asym.)
	1413	C-H (def. sym.)
	1377	C-N (stretch.)
	1325	C-H (def. in plane)
	1262	C-H (def. in plane)
	1148	C-O (stretch.)
	1115	C-O-C (ether.)
	1092	C-O-C (ring)
	1040	C-O (stretch.)
	931	C-H (def. out plane)
	897	C-H (def. out plane)

NA 860 type, equipped with a FT Raman module, a product of NICOLET, USA.

The following measuring parameters were applied: range – 4000 - 100 cm<sup>-1</sup>, resolution – 8 cm<sup>-1</sup>, number of scans – 500, source of radiation – NdYag 1064 nm, energy source – 0.6 W, detector – InGaAs, beamsplitter – CaF<sub>2</sub> [41].

## Results and discussion

In the Raman technique the most intensive bands come from the symmetric non-polar oscillators such as C-C, C=C, S-S, C-S [43 - 46, 48, 50, 51].

For all the fibre samples under investigation FT Raman spectra were prepared. To analyse the spectra characteristic oscillation bands of the groups for dibutrylchitin, krill chitin and Vanson chitosan were determined and next described in the spectrum range 1800 - 820 cm<sup>-1</sup>, presented in **Figure 2.a - 2.c** and **Table 1**.

In order to carry out a quantitative analysis of both the alkaline treatment of DBC fibres transformed into regenerated chitin

fibres as well as of the successive stage of the treatment leading to chitosan fibres, FT Raman spectra distributions were made in the range 1800 - 820 cm<sup>-1</sup> using “GRAMS” software, by Thermo Scientific. To start mathematical processing of the spectra, the optimum function describing Raman bands was selected by preparing a distribution of the spectrum pattern of sulphur as a Raman standard for bands which do not overlap each other.

**Figure 3** demonstrates the band distribution at 472cm<sup>-1</sup> for a symmetric band, whereas **Figure 4** shows the band distribution at 153 cm<sup>-1</sup> for an asymmetric band.

The band distributions were performed using various mathematical functions (Pearson VII, Gauss, Lorentz, Log-Normal, Gauss-Lorentz) included in the “GRAMS” software, by Thermo Scientific. As a result of the mathematical processing, the band areas calculated and the area of the basic band were compared, and the differences evaluated. In

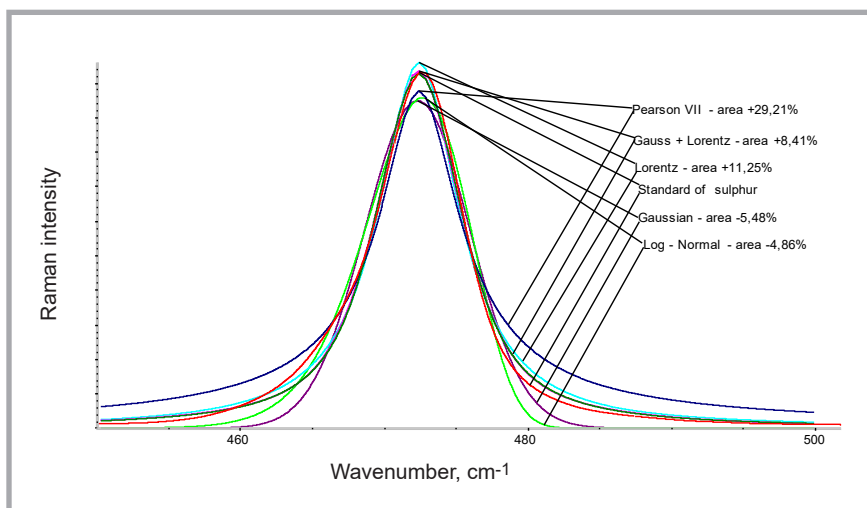


**Figure 3.** Distribution of the Raman band of the Raman shift of sulphur at 472 cm<sup>-1</sup> performed. The areas resulting from the band distribution are compared with that of the basic band.

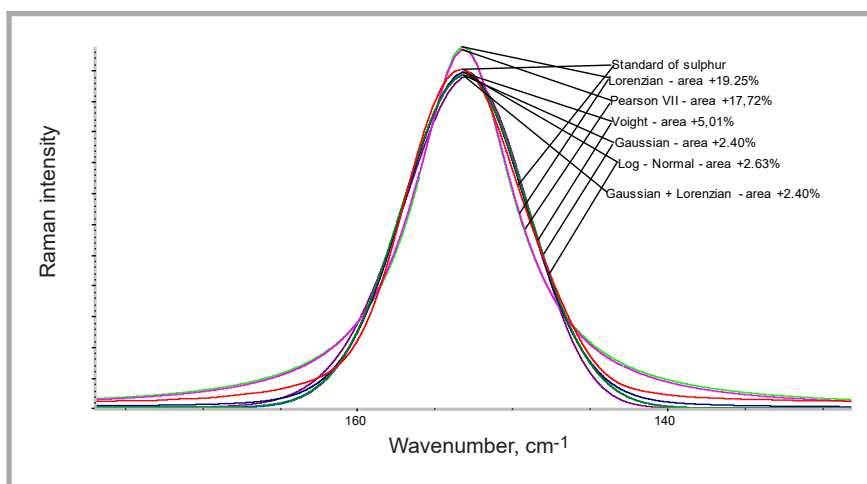


**Figure 4.** Distribution of the Raman band of the Raman shift of sulphur at 153 cm<sup>-1</sup> performed. The areas resulting from the band distribution are compared with that of the basic band.

the case of the symmetric bands a satisfactory correlation (4.86%) was obtained using the Log–Normal function, whereas the application of the Pearson VII function gave the worst correlation of 29.21%. For the asymmetric bands a better correlation resulted from the application of the Gauss and Gauss-Lorentz functions (2.40%) and the worst correlation

was noted for the Pearson VII (17.72%) and Lorentz (19.25%) functions.

Such an initial mathematical processing of the symmetric and asymmetric bands for the standard spectrum made it possible to select mathematical functions adequate to the FT Raman spectra distributions obtained.

Analysis of the first stage of the alkaline treatment of DBC fibres transformed into regenerated chitin fibres using Raman spectroscopy revealed its efficiency and influence on changes in the conformation of the polymer chains obtained.

The Raman spectrum of the DBC fibres is characterised by an intensive band coming from the oscillator C=O of the ester group at 1798 cm<sup>-1</sup>. The band is a basic parameter to determine the esterification degree of chitin.

In all the samples examined, the amide I band can be found with a strongly polarised oscillator C=O as the main constituent. The band can be considered as being without hydrogen interactions, whereas in the hydrogen bond it can be treated as an oscillator with a big symmetry (>C=O···H-O-). The band proportions should thus be shifted towards the lower energies.

In order to activate Raman emission, it is necessary to make the molecular oscillator vibrate. Very often it results in temperature growth, which in extreme cases can lead to the burning of the sample. If the temperature of the sample is too high, hydrogen bonds can be broken, and the maximum emission of the Amide I band can be shifted towards higher energies, characteristic for the free C=O groups.

The proportions of all the bands remain unchanged, except for krill chitin, characterised by a high molecular weight and high level of ordering. The proportions of the bands prove that the deesterification reaction in 5% KOH causes no polymer degradation in the range of the temperature and time applied.

**Figure 5** shows some examples of the Raman spectra distributions made for DBC fibres and for fibres after alkaline treatment at 20 °C in 5% KOH samples

**Table 2.** Degree of butyrylation values for DBC fibres and regenerated chitin fibres (series A - obtained from alkaline treatment of DBC fibres at 20 °C, treatment time: A1 – 10 min, A2 – 20 min, A3 – 30 min, A4 – 60 min) obtained by Raman spectra.

Sample	Alkaline treatment, min	Raman intensity		Spectral coefficient -F >C=O/-C-N	Degree of butyrylation, %	Area of peak >C=O at 1798 cm <sup>-1</sup>	Area of peak -C-N at 1375 cm <sup>-1</sup>	Spectral coefficient -F >C=O/-C-N	Degree of butyrylation, %
		>C=O at 1798 cm <sup>-1</sup>	-C-N at 1375 cm <sup>-1</sup>						
DBC	-	0.074	0.081	0.9136	100.00	2.64	3.17	0.8320	100.00
A1	10	0.055	0.073	0.7534	82.20	1.90	2.61	0.7280	87.50
A2	20	0.074	0.110	0.6727	73.50	2.47	4.14	0.5980	71.90
A3	30	0.039	0.114	0.3421	37.40	1.25	5.50	0.2271	27.30
A4	60	0.000	0.096	0.000	0.00	0.00	3.19	0.0000	0.00

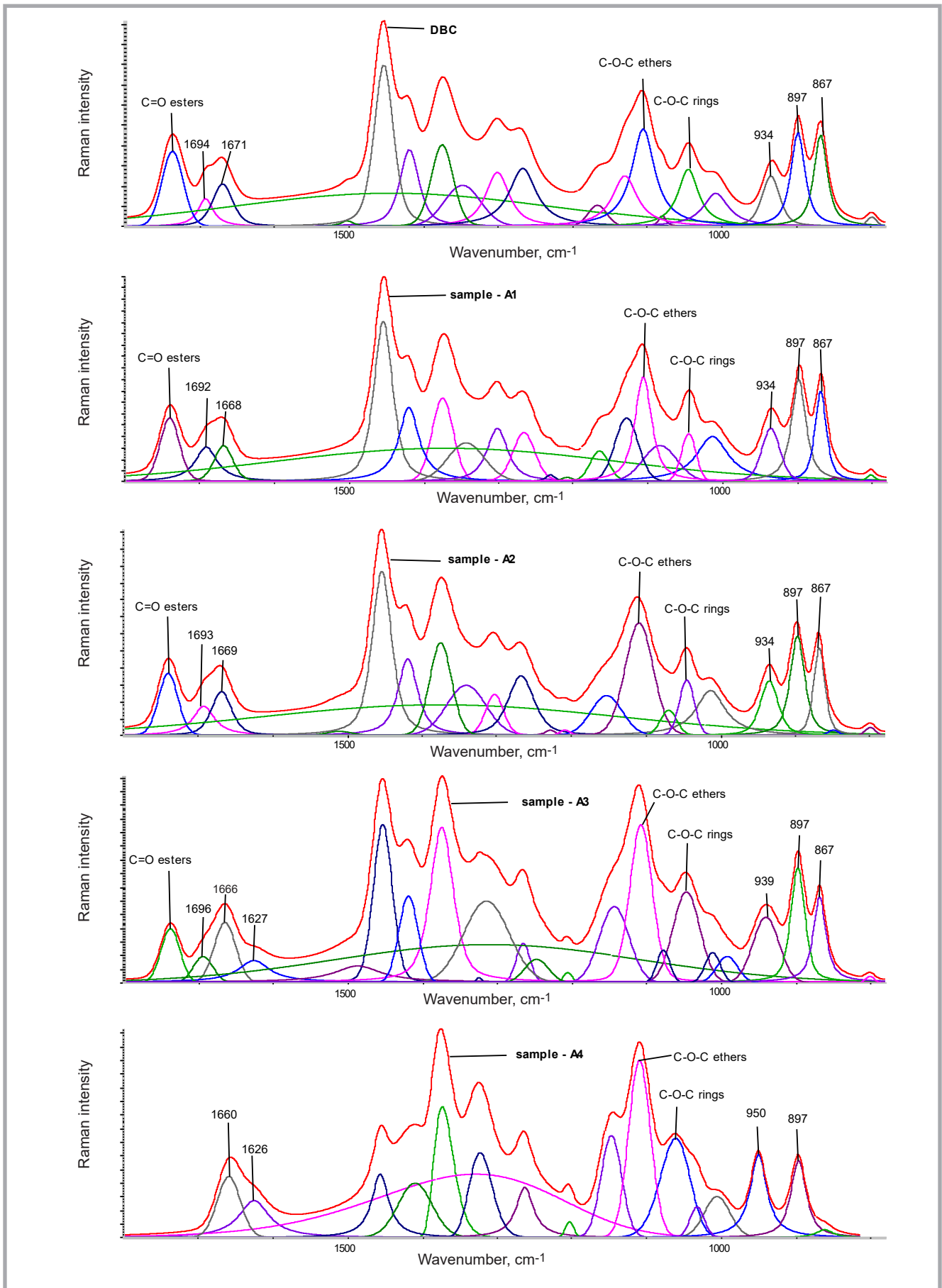


**Figure 5.a.** Sets of FT Raman spectra distributions within the range 1800 – 780  $\text{cm}^{-1}$  of the Raman shift for untreated DBC fibres and for the fibres after alkaline treatment at 20 °C in 5% KOH samples: A1 – after 10 min, A2 – after 20 min, A3 – after 30 min, A4 – after 60 min, (GRAMS software, by Thermo Scientific). **Figure 5.b** see page 32.



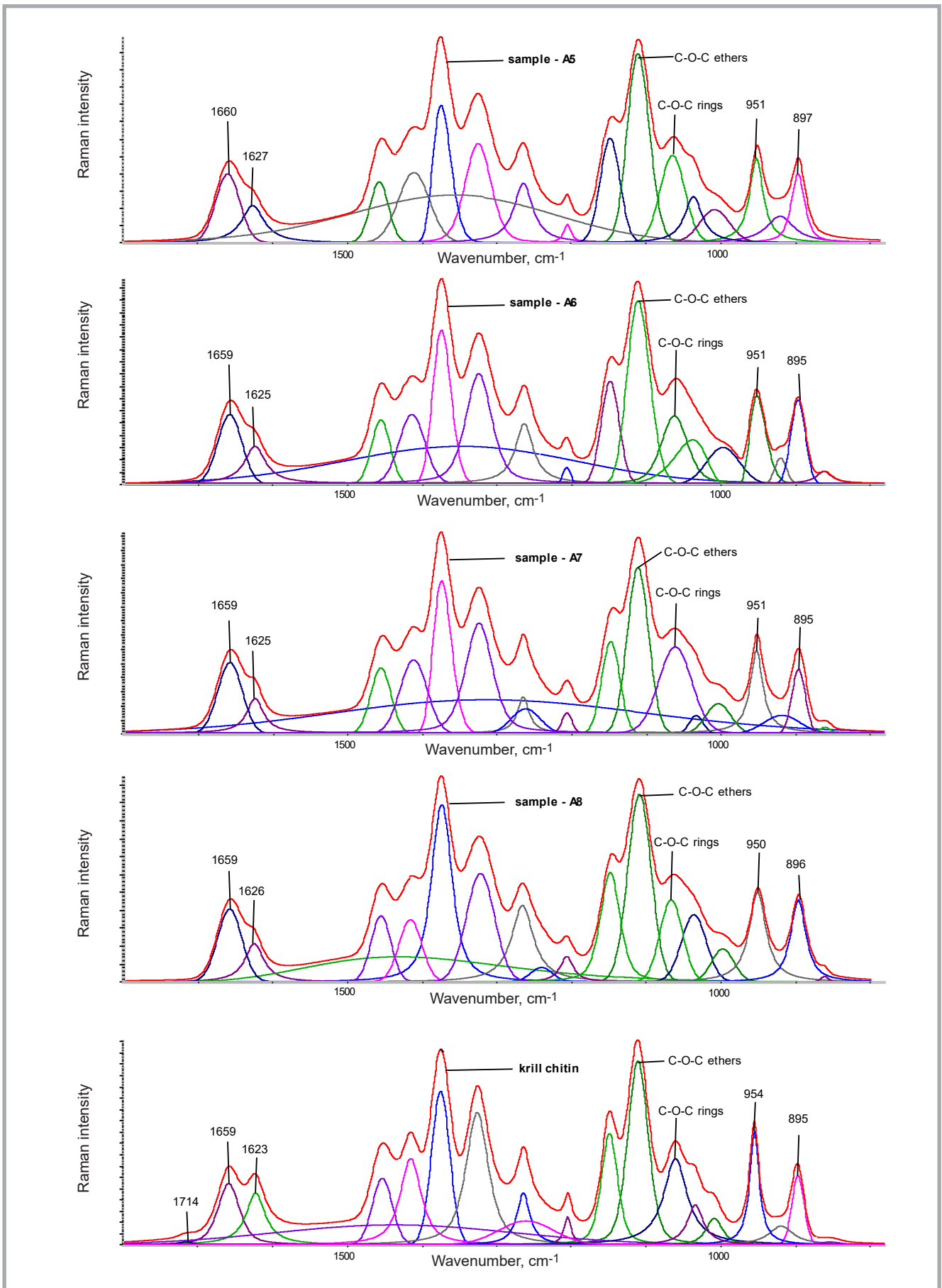


**Figure 5.b.** Sets of FT Raman spectra distributions within the range 1800 – 780 cm<sup>-1</sup> of the Raman shift for the fibres after alkaline treatment at 20 °C in 5% KOH samples: A5 – after 120 min, A6 – after 240 min, A7 – after 480 min, A8 - after 960 min and for krill chitin (GRAMS software, by Thermo Scientific).

using “GRAMS” software, by Thermo Scientific.

Based on the proportions of the band areas calculated for the particular oscillators, the course of the deesterification process and changes in the polymer conformation were analysed, making it possible to calculate the degree of butyrylation of the DBC fibres subjected to alkaline treatment. The results are given in **Table 2**.

Spectral coefficients for the particular spectra were determined both from the absorbance and from the area of the  $-C=O$  band at  $1798\text{ cm}^{-1}$  in relation to the area of the unchanged band  $-C-N$  at  $1375\text{ cm}^{-1}$ .

The values obtained for the DBC fibres were regarded as the standard, with a debutyrylation degree equal to 100%. It is worth mentioning that the debutyrylation degree values calculated from the absorbance and from the band areas are close to those values for samples from the initial

$$WS_i = S_i / (S_{C-N} (\sim 1375\text{ cm}^{-1}) + S_{C-O-C\text{ ether.}} (\sim 1115\text{ cm}^{-1}) + S_{C-O-C\text{ ring.}} (\sim 1092\text{ cm}^{-1})) \quad (1)$$

$$Wh_i = h_i / (h_{C-N} (\sim 1375\text{ cm}^{-1}) + h_{C-O-C\text{ ether.}} (\sim 1115\text{ cm}^{-1}) + h_{C-O-C\text{ ring.}} (\sim 1092\text{ cm}^{-1})) \quad (2)$$

**Equation 1 & 2.**

stage of the alkaline treatment. Slight differences can be observed after 30 min. of the treatment. After 60 min. of the process, both methods of calculations confirm the total deesterification of the DBC fibres. Band proportions for the  $-C-O-C$  oscillators in the heterocyclic ring and oxygen bridges remain unchanged during the alkaline treatment, leading to regenerated chitin, which proves that no polymer degradation takes place in this process.

In order to increase the accuracy of the spectral coefficient determination, it was assumed that the sum of the band areas and their heights for the  $-C-N$  and  $-C-O-C$  oscillators remains stable. Proportional changes for the  $-C-H$  bands were calculated in relation to the sum above.

Changes occurring in the remaining bands were related to the constant values above (**Equation 1, 2**) where,  $WS_i$  - proportionality coefficient of the area of the definite band ( $S_i$ ) in relation to the sum of areas of  $C-N$  ( $S_{C-N} (\sim 1375\text{ cm}^{-1})$ ),  $C-O-C$  ether ( $S_{C-O-C\text{ ether.}} (\sim 1115\text{ cm}^{-1})$ ) &  $C-O-C$  heterocyclic ring ( $S_{C-O-C\text{ ring.}} (\sim 1092\text{ cm}^{-1})$ );  $Wh_i$  - proportionality coefficient of the height of the definite band ( $h_i$ ) in relation to the sum of heights of  $C-N$  ( $h_{C-N} (\sim 1375\text{ cm}^{-1})$ ),  $C-O-C$  ether ( $h_{C-O-C\text{ ether.}} (\sim 1115\text{ cm}^{-1})$ ), &  $C-O-C$  heterocyclic ring ( $h_{C-O-C\text{ ring.}} (\sim 1092\text{ cm}^{-1})$ ) oscillators.

A set of height proportions of the  $C-H$  bands vibrating in the ring plane and outside it in relation to the sum of the heights of the  $C-H$  and  $C-O-C$  bands is shown in **Figures 6 and 7**.

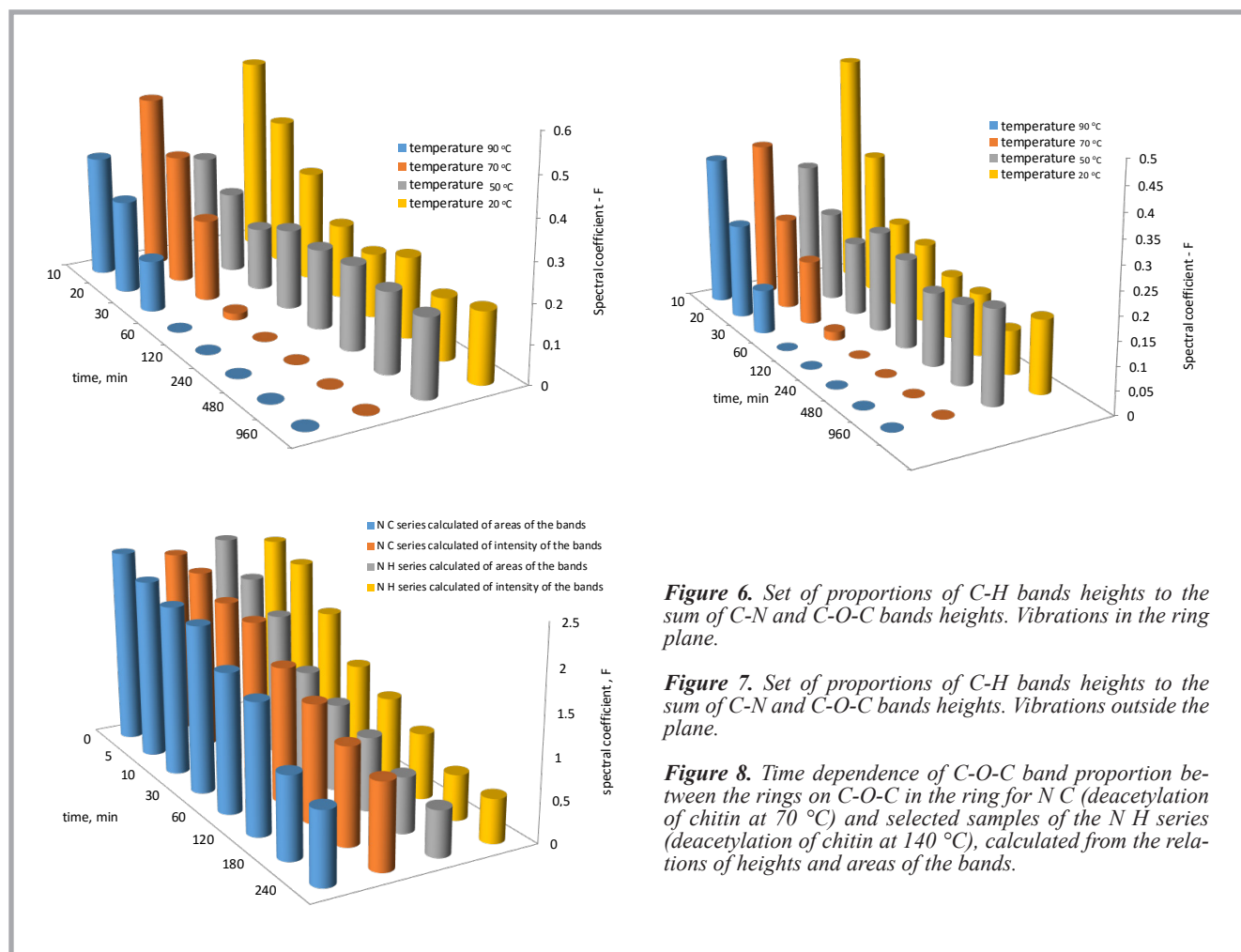


**Figure 6.** Set of proportions of  $C-H$  bands heights to the sum of  $C-N$  and  $C-O-C$  bands heights. Vibrations in the ring plane.

**Figure 7.** Set of proportions of  $C-H$  bands heights to the sum of  $C-N$  and  $C-O-C$  bands heights. Vibrations outside the plane.

**Figure 8.** Time dependence of  $C-O-C$  band proportion between the rings on  $C-O-C$  in the ring for  $N C$  (deacetylation of chitin at  $70\text{ }^\circ\text{C}$ ) and selected samples of the  $N H$  series (deacetylation of chitin at  $140\text{ }^\circ\text{C}$ ), calculated from the relations of heights and areas of the bands.

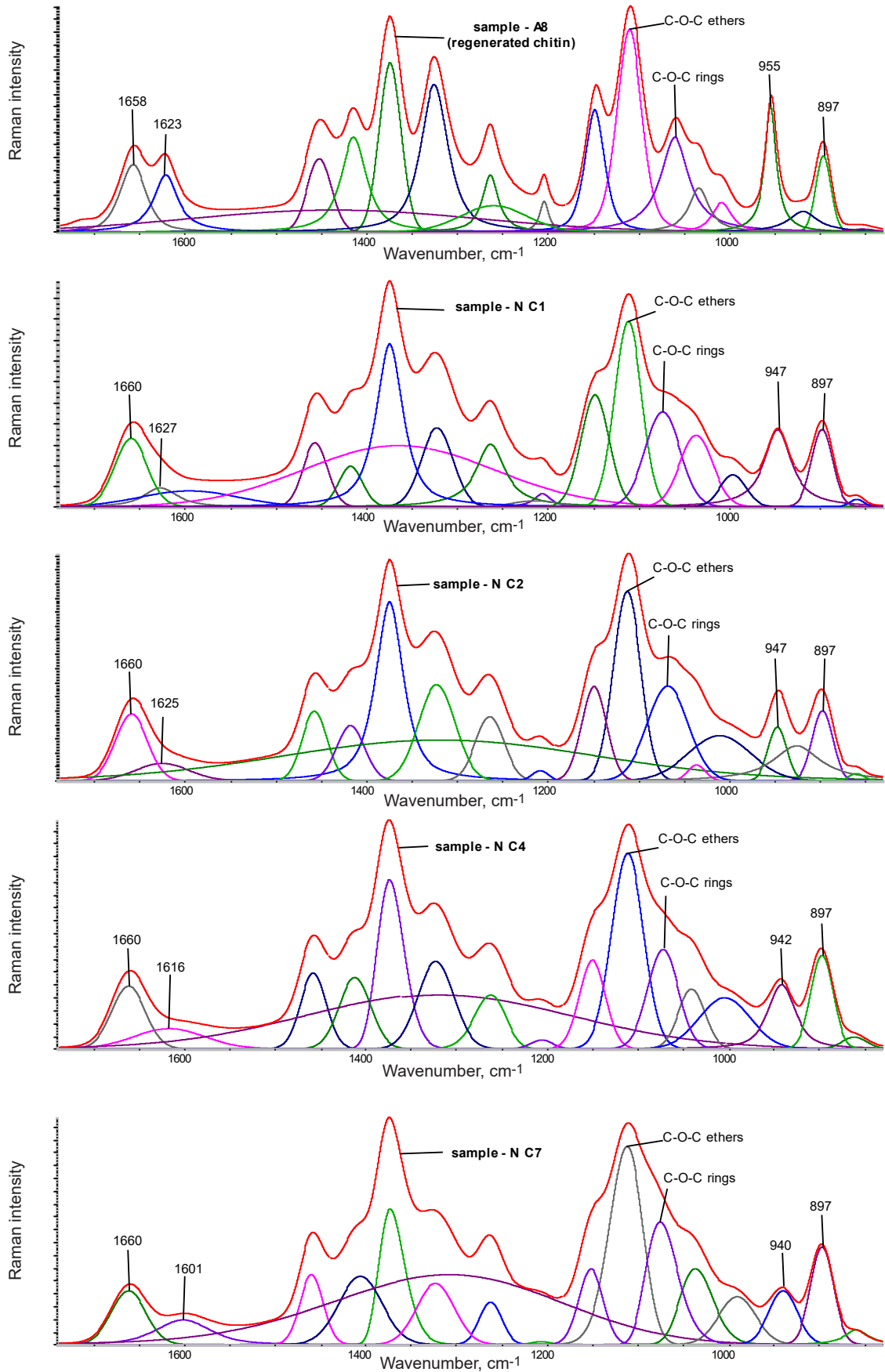


**Figure 9.a.** Sets of Raman spectra distributions within the range 1800 – 780 cm<sup>-1</sup> of the Raman shift for regenerated chitin fibres (sample A8) and for the fibres after deacetylation in saturated KOH at 70 °C, samples: N C2 – after 10 min, N C4 – after 30 min, N C7 – after 60 min.



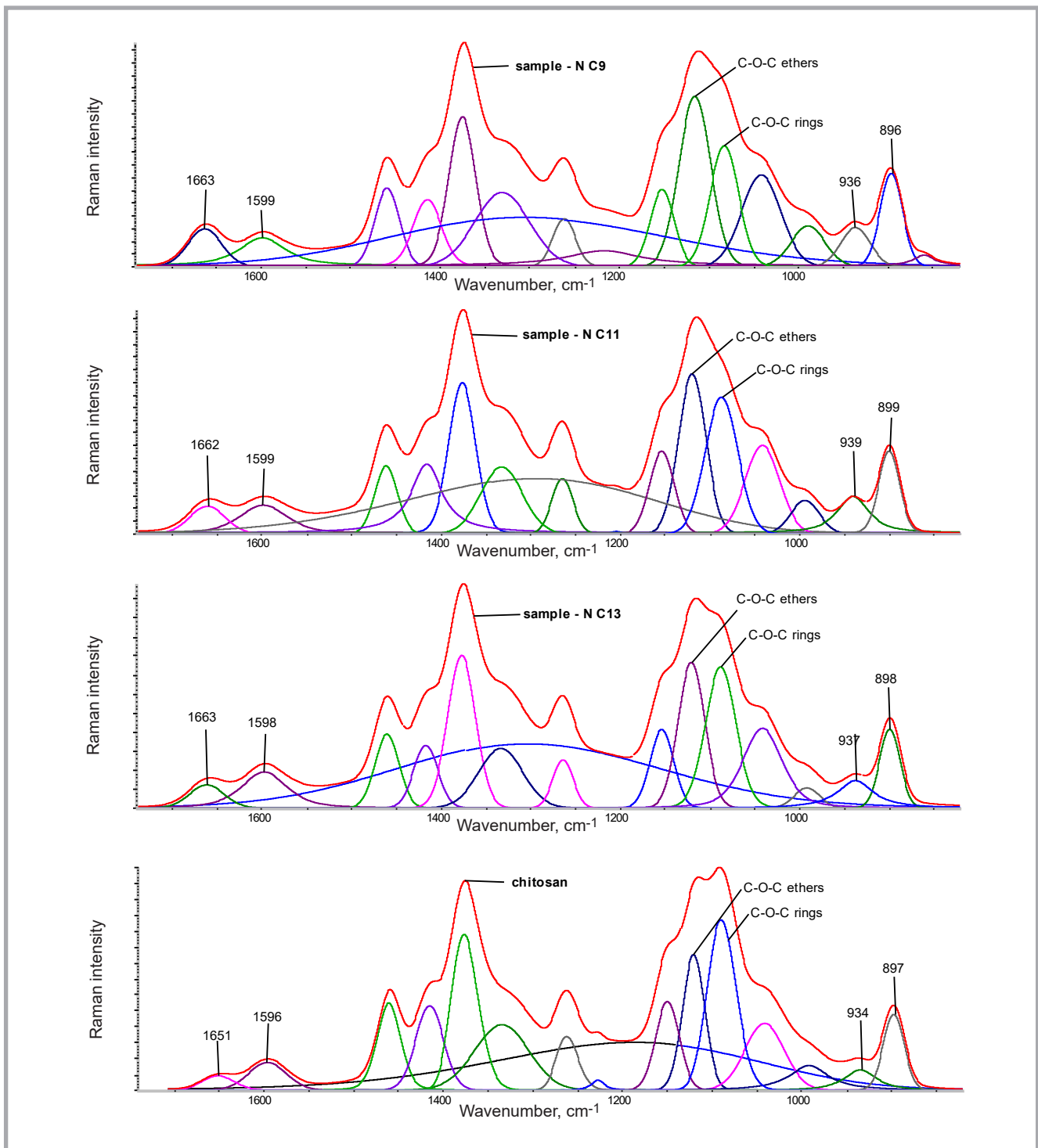


**Figure 9.b.** Sets of Raman spectra distributions within the range  $1800 - 780 \text{ cm}^{-1}$  of the Raman shift for the fibres after deacetylation in saturated KOH at  $70^\circ\text{C}$ , samples: N C9 – after 120 min, N C11 – after 180 min, N C13 – after 240 min, and for chitosan (DD - 90%).

It was observed that as a result of the alkaline treatment of the DBC fibres with 5% KOH at the temperatures applied, a change in the C-H band proportions takes place both in the ring plane and outside it. The higher the temperatures, the more intense. The proportion are changes which finally stabilise.

Under mild conditions of the alkaline treatment, the average distance between

the macromolecules becomes smaller, and thus the formation of hydrogen bonds between the amide and hydroxyl groups is possible. Therefore after the treatment stabilization of the supermolecular structure with a different conformation of the polymer chains takes place.

As mentioned before, the deesterification reaction at temperatures from 20 to

$90^\circ\text{C}$  with a 5% KOH solution causes no degradation of the polymer chains.

However, polymer degradation occurs in the case of chitin deacetylation carried out in saturated KOH solutions at elevated temperatures (at  $70, 100, 120$  and  $140^\circ\text{C}$ ). The process of chitin deacetylation requires more severe conditions, which, on the other hand, cause gradual degradation of the macromolecules.

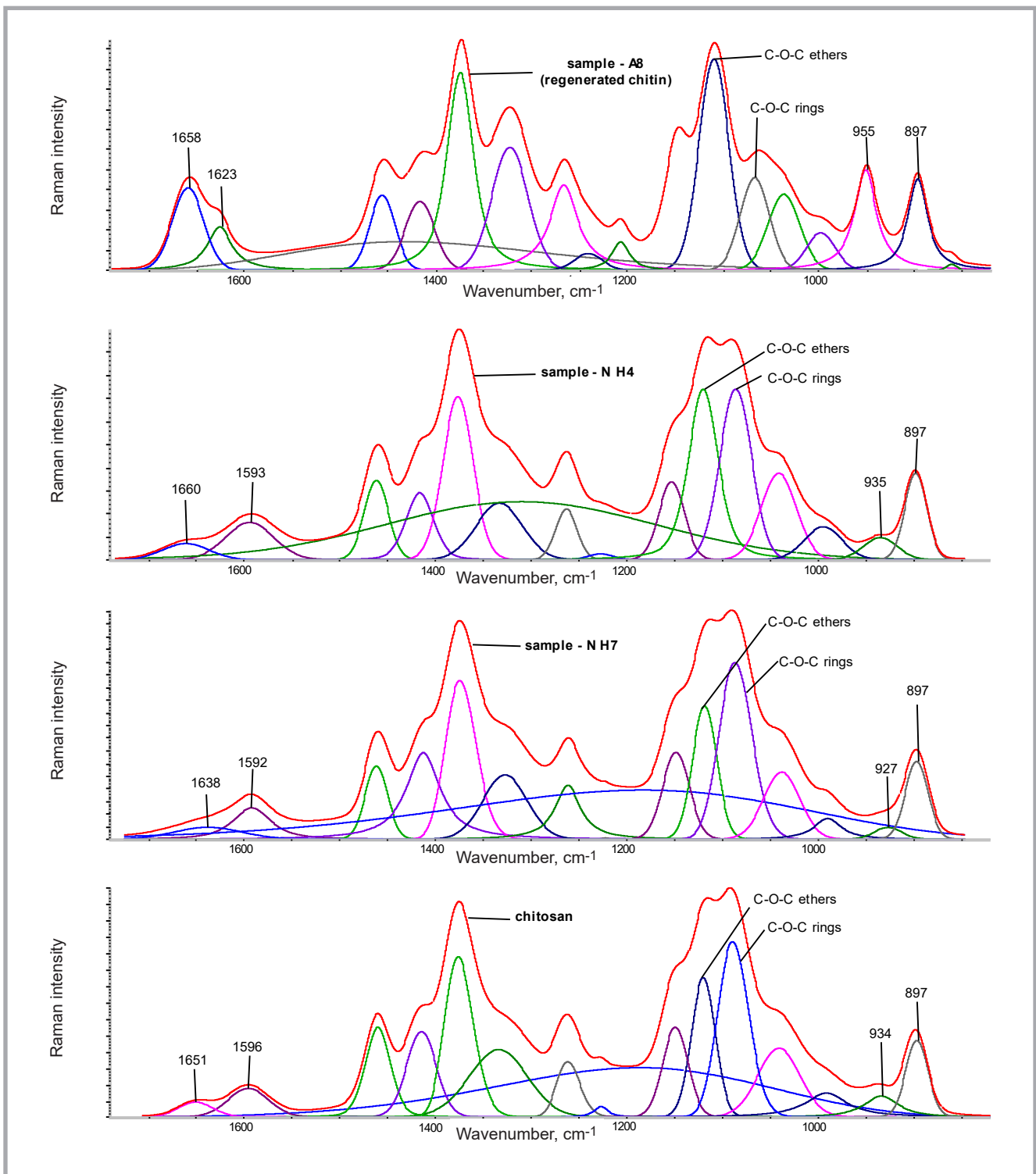


**Figure 10.** Sets of Raman spectra distributions within the range  $1740 - 820 \text{ cm}^{-1}$  of the Raman shift for regenerated chitin fibres (sample A8) and for the fibres after deacetylation in saturated KOH at  $140^\circ\text{C}$ , samples: N H4 – after 60 min, N H7 – after 240 min and for chitosan (DD – 90%).

The degradation phenomenon can easily be observed when the band proportions coming from the C-O-C group in the ring and from the C-O-C groups between the rings are compared. The polymer degradation brings about decomposition of the oxygen bridges between the rings, expressed by the lowering of the ether C-O-C band intensity at  $1115 \text{ cm}^{-1}$  in re-

lation to the C-O-C band in the ring at  $1092 \text{ cm}^{-1}$  in the Raman spectra. The effect of deacetylation on the C-O-C band proportions is presented in **Figure 8** (see page 33).

In order to determine the band parameters of the spectra, their analysis by means of GRAMS software, by Thermo Scientific,

was carried out. A set of the Raman spectra distributions is shown in **Figures 9** (see page 34 & 35) and **10**.

On the basis of the FT Raman band distributions, the deacetylation degree for the NC series (deacetylation - alkaline treatment of chitin fibres at  $70^\circ\text{C}$ ) was calculated, the results of which are pre-

**Table 3.** Deacetylation degree (DD) values for the chitosan fibres (series N C - deacetylation) obtained from the regenerated chitin fibres deacetylated at 70 °C and Vanson chitosan (\*Vanson was determined by potentiometric titration deacetylation degree, DD = 90%).

Sample	Alkaline treatment, min	Raman intensity		Spectral coefficient -F >C=O/-N-H	Degree of deacetylation, %	Area of peak C=O at 1659 cm <sup>-1</sup>	Area of peak -N-H at 1626 cm <sup>-1</sup>	Spectral coefficient -F >C=O/-N-H	Degree of deacetylation, %
		>C=O at 1659 cm <sup>-1</sup>	-N-H at 1626 cm <sup>-1</sup>						
N C1	5	0.04718	0.01218	3.8740	11.5	1.5096	0.5751	2.625	14.4
N C2	10	0.03302	0.00930	3.5510	12.5	2.0788	0.8985	2.314	16.3
N C4	30	0.04920	0.01570	3.1340	14.2	2.2597	1.5360	1.471	25.6
N C7	60	0.04140	0.01932	2.1430	20.7	1.9626	1.7230	1.139	33.1
N C9	120	0.02880	0.02270	1.2690	35.0	1.3624	1.8645	0.731	51.6
N C11	180	0.02124	0.02230	0.9525	46.6	1.0584	1.6745	0.632	59.7
N C13	240	0.02370	0.03840	0.6172	72.0	1.1440	3.0050	0.381	98.9
Vanson*	-	0.08650	0.17530	0.4340	90.0	3.8480	9.1880	0.419	90.0

sented in **Table 3**. Spectral coefficients for the particular spectra were determined. As the standard, Vanson chitosan with the determined (by potentiometric titration) deacetylation degree was applied. The values of the spectral coefficient were calculated both from the absorbance and from the -C=O band area at 1659 cm<sup>-1</sup> in relation to the -NH band area at 1626 cm<sup>-1</sup>. However, the deacetylation degrees of the fibres calculated by means of the two methods above differ significantly from each other, which is probably caused by the method of the mathematical treatment of the Raman spectra applied. Thus Raman spectroscopy creates no possibility to evaluate the deacetylation degree with the accuracy of NIR spectroscopy within the range of the wave number from 10,600 to 5,600 cm<sup>-1</sup> [51].

## Conclusions

It was found out that in the course of the partial deesterification (debutyrylation) of dibutrylchitin fibres to the regenerated chitin fibres no changes in the band proportions of the symmetric oscillators for amide and ether groups take place either in the ring plane or outside it the plane. If the process is carried out under mild conditions, no degradation of the polymer chains is observed.

Transformations of the C-H oscillators vibrating both in the ring plane and outside it the plane confirm the changes in the polymer chain conformation taking place during the deesterification of dibutrylchitin fibres.

The a analysis of the further deesterification and deacetylation of the obtained fibres obtained carried out by means of RAMAN spectroscopy proves that in the process probably gradual degradation of the polymer chains probably takes place.

Raman spectroscopy has also been used to establish differences in the structure and the degree of substitution of chitin, chitosan and dibutrylchitin.

## References

- Muzzarelli RAA and Muzzarelli C. Chitosan chemistry: relevance to the biomedical sciences. *Advances in Polymer Science* 2005; 186: 151–209.
- Muzzarelli RAA, Guerrieri M, Goteri G, Muzzarelli C, Armeni T, Ghiselli R and Cornellisen M. The biocompatibility of dibutryl chitin in the context of wound dressings. *Biomaterials* 2005, 26: 5844–5854.
- Rinaudo M. Chitin and chitosan: properties and applications. *Progress in Polymer Science* 2006; 31: 603–632.
- Kumar MNVR. A review of chitin and chitosan applications. *Reactive and Functional Polymers* 2000; 46(1): 1–27.
- Villetti MA, Crespo JS, Soldi MS, Pires ATN, Borsali R and Soldi V. Thermal Degradation of Natural Polymers. *Journal of Thermal Analysis and Calorimetry* 2002; 67(2): 295–303.
- Kurita K. Controlled functionalization of the polysaccharide chitin. *Progress in Polymer Science* 2001; 26: 1921–1971.
- Pillai CKS, Paul W and Sharma ChP. Chitin and chitosan polymers: Chemistry, solubility and fiber formation. *Progress in Polymer Science* 2009; 34: 641–678.
- Hemant KSY, Shivakumar HG. Development of chitosan acetate films for transdermal delivery of propranolol hydrochloride. *Tropical Journal of Pharmaceutical Research* 2010; 9(2): 197–203.
- Shu XZ and Zhu KJ. The influence of multivalent phosphate structure on the properties of ionically cross-linked chitosan films for controlled drug release. *European Journal of Pharmaceutics and Biopharmaceutics* 2002; 54: 235–243.
- Silva CL, Pereira JC, Ramalho A, Pais ACC, Sousa JS. Films based on chitosan polyelectrolyte complex for skin drug delivery: development and characterization. *Journal of Membrane Science* 2008; 320: 268–279.
- Kofuji K, Ito T, Murata Y and Kawashima S. The controlled release of a drug from biodegradable chitosan gel beads. *Chemical & Pharmaceutical Bulletin* 2000; 48(4): 579–581.
- Martinez-Ruvalcaba A, Schanchez-Diaz JC, Becerra F and Cruz-Barba LE. Swelling characterization and drug delivery kinetics of polyacrylamide-coitaconic acid/chitosan hydrogels. *eXPRESS Polymer Letters* 2009; 3(1): 25–32.
- Hirano S. Water-soluble glycol chitin and carboxymethylchitin. *Methods in Enzymology* 1988; 161: 408–410.
- Lim SH and Hudson SM. Review of chitosan and its derivatives as antimicrobial agents and their uses as textile chemicals. *Journal of Macromolecular Science-Polymer Reviews*. 2003; C43: 223–269.
- Sini TK, Santhosh S and Mathew PT. Study of the influence of processing parameters on the production of carboxymethylchitin. *Polymer* 2005; 46(9): 3128–3131.
- Szosland L, Janowska G. The method of preparation of dibutrylchitin. *Polish Patent PL 169077B1*; 1996.
- Szosland, L. Di-O-butyrylchitin. In Muzzarelli RAA, Peter M G (Eds.), *Chitin Handbook* 1997; (53–60), Italy: Atec.
- Szosland L. Synthesis of highly substituted butyrylchitin in the presence of perchloric acid. *Journal of Bioactive and Compatible Polymers* 1996; 11: 61–71.
- Biniaś D, Boryniec S and Biniaś W. Dibutrylchitin Fibres Formed from Ethylen Alcohol Solutions. *Progress on Chemistry and Application of Chitin and its Derivatives*. 2003 (Monograph.Vol. IX) Henryk Struszczyk (Eds.) Lodz, Polish Chitin Society; 161–168.
- Biniaś D, Boryniec S and Biniaś W. Studies on the structure of polysaccharides in the process of alkaline treatment of dibutrylchitin fibres. *Fibres and*

- Textiles in Eastern Europe* 2005; 13(5): 137-140.
21. Wlochowicz A, Szosland L, Binias D and Szumilewicz J. Crystalline structure and mechanical properties of wet-spun dibutylchitin fibers and products of their alkaline treatment. *Journal of Applied Polymer Science* 2004; 94(5): 1861-1868.
  22. Szosland L, Krucińska I, Cisko R, Paluch D, Staniszevska-Kuś J, Solski L and Szymonowicz M. Synthesis of dibutylchitin and preparation of new textiles made from dibutylchitin and chitin for medical applications. *Fibres and Textiles in Eastern Europe* 2001; 9, 3(34): 54-57.
  23. Paluch D, Szosland L, Kołodziej J, Staniszevska-Kuś J, Szymonowicz M, Solski L and Zywiecka B. Biological investigation of the regenerated chitin fibers. *Engineering of Biomaterials* 1999; II: 52-60.
  24. Paluch D, Pielka S, Szosland L, Kołodziej J, Staniszevska-Kuś J, Szymonowicz M, and Solski L. A biological investigation of dibutylchitin fibres. *Engineering of Biomaterials* 2000; III: 17-22.
  25. Pielka S, Paluch D, Staniszevska-Kuś J, Zywicka B, Solski L, Szosland L, Czarny A and Zaczyńska E. Wound healing accelerating by a textile dressing containing dibutylchitin and chitin. *Fibres and Textiles in Eastern Europe* 2003; 11, 2(41): 79-84.
  26. Muzzarelli C, Francescangeli O, Tosi G and Muzzarelli RAA. Susceptibility of dibutyl chitin and regenerated chitin fibres to deacetylation and depolymerization by lipases. *Carbohydrate Polymers* 2004; 56: 37-146.
  27. Chilarski A, Szosland L, Krucińska I, Kiekens P, Błasińska A, Schoukens G, Cisko R, Szumilewicz J. Novel dressing materials accelerating wound healing made from dibutylchitin. *Fibres and Textiles in Eastern Europe* 2007; 4(63): 77-81.
  28. Schoukens G, Kiekens P and Krucinska I. New bioactive textile dressing materials from dibutylchitin. *International Journal of Clothing Science and Technology* 2009; 21(2/3): 93 - 101.
  29. Krucinska I, Komisarczyk A, Paluch D, Szymonowicz M, Zywicka B and Pielka S. The impact of the dibutylchitin molar mass on the bioactive properties of dressings used to treat soft tissue wounds. *J Biomed Mater Res Part B* 2012; 100B:11-22.
  30. Błasińska A and Drobnik J. Effects of non-woven mats of di-O-butylchitin and related polymers on the process of wound healing. *Biomacromolecules* 2008, 3, vol. 9, 776-782.
  31. Błasińska A and Kun T. Influence of dibutylchitin on histamine release from mast cells. *Progress on Chemistry and Application of Chitin and Its Derivatives* ed. by M.M.Jaworska, Łódź-Poland, 2008, 95-106.
  32. Domszy JG and Roberts GAF. Evaluation of infrared spectroscopic techniques for analysing chitosan. *Die Makromolekulare Chemie* 1985; 186: 1671-1677.
  33. Focher B, Naggi A, Torri G, Cosani A and Terbojevich M. Structural differences between chitin polymorphs and their precipitates from solutions-evidence from CP-MAS <sup>13</sup>C-NMR, FT-IR and FT-Raman spectroscopy. *Carbohydrate Polymers* 1992; 17(2): 97-102.
  34. Brugnerotto J, Lizardi J, Goycoolea FM, Argüelles-Monal W, Desbrieres J and Rinaudo M. An infrared investigation in relation with chitin and chitosan characterization. *Polymer* 2001; 42 3569-3580.
  35. Yamaguchi Y, Nge TT, Takemura A, Hori N and Ono H. Characterization of uniaxially aligned chitin film by FT-IR spectroscopy. *Biomacromolecules* 2005; 6:1941-1947.
  36. Kumirska J, Czerwicka M, Kaczyński Z, Bychowska A, Brzozowski K, Thöming J and Stepnowski P. Application of Spectroscopic Methods for Structural Analysis of Chitin and Chitosan. *Marine Drugs* 2010; 8 (5): 1567-1636.
  37. Prabu K, Natarajan E. Isolation and FTIR spectroscopy characterization of chitin from local sources. *Advances in Applied Science Research* 2012; 3(2): 1870-1875.
  38. Van De Velde K, Kiekens P. Structure analysis and degree of substitution of chitin, chitosan and dibutylchitin by FT-IR spectroscopy and solid state <sup>13</sup>C NMR. *Carbohydrate Polymers* 2004; 58: 409-416.
  39. Binias D, Boryniec S, Binias W and Wlochowicz A. Changes in structure of dibutylchitin fibres in process of chitin regeneration. *Polimery* 2005; 50(10): 742-747.
  40. Binias D, Boryniec S, Binias W and Wlochowicz A. Alkaline treatment of dibutylchitin fibers spun from polymer solution in ethyl alcohol. *Fibres & Textiles in Eastern Europe* 2006; 14(3): 12-18.
  41. Binias D, Wyszomirski M., Binias W and Boryniec S. Supermolecular structure of chitin and its derivatives in FTIR spectroscopy studies. *Progress on Chemistry and Application of Chitin and Its Derivatives* ed. by M.M. Jaworska, Łódź-Poland, 2007, 95-108.
  42. Binias W, Binias D. Application of FTNIR Spectroscopy for evaluation of the degree of deacetylation of chitosan fibres. *Fibres & Textiles in Eastern Europe* 2015; 23, 2(110): 10-18.
  43. Galat A, Popowicz J. Study of the Raman scattering spectra of chitins, *Bulletin Academy Polonian Sciences, Series Science Biology* 1978; 26(8): 519-524.
  44. De Gussem K, Vandenabeele P, Verbeken A, Moens L. Raman spectroscopic study of Lactarius spores (Russulales, Fungi). *Spectrochimica Acta Part A: Molecular and Biomolecular Spectroscopy* 2005; 61: 2896-2908.
  45. Ehrlich H, Maldonado M, Spindler K-D, Eckert C, Hanke T, Born R, Goebel C, Simon P, Heinemann S and Worch H. First Evidence of Chitinase Component of the Skeletal Fibers of Marine Sponges. Part I. Verongidae (Demospongia: Porifera) *Journal of experimental zoology* 2007; 308B: 347-356.
  46. Ehrlich H, Kaluzhnaya O V, Brunner E, Tsurkan MV, Ereskovsky A, Ilan M, Tabachnick KR, Bazhenov VV, Paasch S, et al. Identification and first insights into the structure and biosynthesis of chitin from the freshwater sponge *Spongilla lacustris*. *Journal of Structural Biology* 2013; 183 (3): 474-483.
  47. Ehrlich H, Kaluzhnaya OV, Tsurkan MV, Ereskovsky A, Tabachnick KR, Ilan M, Stelling A, Galli R, Petrova OV, Nekipelov SV, Sivkov VN, Vyalikh D, Born R, Behm T, Ehrlich A, Chernogor L I, Belikov S, Janussen D, Bazhenov VV and Wörheide G. *First report on chitinous holdfast in sponges (Porifera). Proceedings of the Royal Society B* 2013; 280.
  48. Wysokowski M, Bazhenov VV, Tsurkan MV, Galli R, Stelling AL, Stöcker H and Kaiser S. Isolation and Identification of chitin in three-dimensional skeleton of *Aplysina fistularis* marine sponge. *International Journal of Biological Macromolecules* 2013; 62: 94-100.
  49. Brzeski M, Mieczkowska M, Sowa K, Stolz H, Wojtasz-Pająk A and Neugebauer W. Technologia otrzymywania chityny z pancerzy kryla antarktycznego, *Studia i Materiały Seria S* 1985; WMIR, Gdynia; (2): 13-23.
  50. Socrates G. *Infrared and Raman characteristic group frequencies*, (3<sup>rd</sup> Ed.) 2001; England: John Wiley&Sons Ltd.
  51. Siesler HW, Ozaki Y, Kawata S and Heise HM. *Near-Infrared Spectroscopy* 2002 (Principles, Instruments, Applications); WILEY-VCH Weinheim (Germany).